**RESEARCH ARTICLE**

# Experimental Validation of a Mitigation Method of Ferranti Effect in Transmission Line

**TAREQ FOQHA**[1]**, SAMER ALSADI**[1]**, (Senior Member, IEEE),**
**SHADY S. REFAAT**[2,3]**, (Senior Member, IEEE),**
**AND KAIS ABDULMAWJOOD**[2,4]**, (Senior Member, IEEE)**

[1]Electrical Engineering Department, Palestine Technical University–Kadoorie, Tulkarm P304, Palestine
[2]Electrical and Computer Engineering Department, Texas A&M University at Qatar, Doha, Qatar
[3]School of Physics, Engineering and Computer Science, University of Hertfordshire, AL10 9EU Hatfield, U.K.
[4]University of Ontario Institute of Technology (UOIT), Oshawa, ON L1G 0C5, Canada

Corresponding author: Kais Abdulmawjood (kais.abdulmawjood@qatar.tamu.edu)

**ABSTRACT** Electric power transmission networks should be operated in efficient, safe, and reliable conditions. To improve the stability and transfer capability of power transmission, it is necessary to mitigate the Ferranti effect. This paper investigates the impact of increasing the length of the transmission line on its receiving end voltage under no-load conditions. A variable shunt reactor compensation for transmission lines is used to control the voltage level at different lengths of the transmission line. The proposed method demonstrates that the value of the shunt reactor required to maintain the receiving end voltage can be estimated. Moreover, the system is modeled using the PowerWorld simulator, and the effectiveness of the proposed model has been verified by experimental results. The experimental results demonstrate the efficiency of the proposed methodology and match the simulation results, which are then validated by simulating the WSCC 9-bus and IEEE 30-bus test systems.

**INDEX TERMS** Transmission lines, ferranti effect, shunt compensation, powerworld simulator.

## I. INTRODUCTION

A transmission network function transmits electric energy from various power sources to the system, which ultimately supplying the load. Overhead transmission lines are preferred over underground cables. Overhead lines may significantly reduce the cost of providing vast amounts of electricity, and their maintenance costs and procedures are significantly more straightforward and uncomplicated than underground cables [1], [2].

The skin effect, proximity effect, corona discharge, and Ferranti effect are influenced factors for electrical transmission lines [3]. Corona effect is an effect of violet glow, hissing noise, and production of ozone gas in a high voltage overhead transmission line. Since the formation of the corona causes energy loss, some part of valuable energy gets reduced due to this phenomenon, which is very harmful to transmission

The associate editor coordinating the review of this manuscript and approving it for publication was Youngjin Kim[ID].

systems [4], [5], [6]. Skin effect is an alternating current that tends to flow through the surface of transmission lines conductors that leads to ac losses [7], [8], and a phenomenon known as the proximity effect occurs when conductors carrying alternating current are close to one another. A circulating current will begin to flow in the conductor as a result of this alternating flux, leading to a non-uniform distribution of current along the transmission line, which raises the conductor's apparent resistance and results in a voltage drop and power loss [9], [10]. Ferranti effect is a phenomenon that occurs when one end of a long transmission line is energized while the other end is unloaded or lightly loaded [11], [12]. Ferranti effect has adverse effects on the system which include; equipment damage. Their windings can burn because of high voltage, which reduces the power system power factor leading to instability of the power system.

Due to the capacitive effect of the line, the receiving voltage becomes higher than the sending voltage during no-load or light-load conditions. In this situation, reactive power

generated exceeds reactive power absorbed. Consequently, it damages the connected loads [13], [14], [15]. Therefore, developing an effective mitigation method of the Ferranti effect in transmission lines plays a crucial role in improving the stability, efficiency, and transfer capability of the power transmission aspect.

Different methods have been developed for mitigation Ferranti effect. In [16], the authors have used the Thyristor Controlled Reactor (TCR) and fixed inductor to reduce the Ferranti effect. Simulations were performed in MATLAB software at no load and light load conditions at various lengths of the line. The purpose was to determine the effect of increasing the line length on the receiving end voltage. A comparison between the use of a fixed inductor and a TCR to mitigate the Ferranti impact is then performed. It was found that the receiving end voltage of the line increases gradually as the line length increases. The voltage is brought within the range by using a fixed inductor and TCR. The disadvantage of using a fixed inductor is that it acts as a load even when there is no light load/no load condition, and the main disadvantage of using TCR is that it introduces harmonics into the system.

Chavan et al. [12], discussed a novel application of the Static Series Synchronous Compensator (SSSC) connected in series with the transmission line to mitigate the Ferranti effect. The Power System Computer Aided Design (PSCAD) is used to design the system, which includes a two-level Voltage Source Converter based SSSC with slightly modified controls. When the SSSC was turned on, the voltage was reduced at the receiving end. The line's reactive power requirement was also reduced, and it was more effective at compensating voltage for inductive loads than resistive loads.

In [17], the issues with high voltage stability in India's western regional grid are described, as well as mitigation techniques such as dynamic compensation and static synchronous compensation in the system. It was found that the STATCOM is the most appropriate dynamic compensation in a system, which results in a reactive power balance in the system. As a result, the problem of voltage stability is solved.

In [18], the impact of the installed 400 kV shunt reactors on Oman grid is described. The shunt reactors are installed to limit the voltage rise in the grid during light loading conditions in winter period. The recorded actual voltages and reactive power verified the effectiveness of the shunt reactors in improving voltage profile and shifting the operating points of generators into more stable region.

The reactive power available at a given point in a transmission system determines the voltage stability at that point. Reactive power is an essential parameter in electric power systems because it impacts their efficiency. The capacitive loads can produce overvoltage, which causes insulation failure in electrical conductors and overvoltage in electric transformers due to the Ferranti effect. This results in poor power quality. Therefore, it is essential to monitor reactive power as accurately as possible [19], [20].

Reactive power compensation is approached from two aspects: load compensation and voltage support. The main aim of load compensation is to improve power quality, whereas the objective of voltage support is to reduce voltage fluctuations at transmission line terminals [21], [22].

The present work proposes a new approach for estimating the value of the shunt reactor, which is required to maintain the voltage and improve the performance of the power system under various conditions. PowerWorld simulator is used as the analysis tool. A detailed experimental investigation is carried out in this study to verify the simulation results. To validate the suggested methodology, simulations of the WSCC 9-bus and IEEE 30-bus are performed.

The following points summarize the main contributions of this paper as follows:

- Proposing a new approach for estimating the value of the shunt reactor required to maintain the receiving end voltage of the transmission line and mitigate Ferranti effect.
- Verifying the proposed methodology using experimental results.
- Validating the suggested methodology's effectiveness by applying it to the standard WSCC 9-bus and IEEE 30-bus systems

The rest of this paper is organized as follows. A brief overview of the Ferranti effect, transmission line modeling, and compensation technique for mitigating this effect are discussed in Section II. Section III introduces the methodology for modeling the power system, determining Ferranti effect and estimating the value of the shunt reactor to maintain the bus voltages within the allowable limits. Section IV describes the power system simulation carried out along with the experimental measurements conducted in the laboratory to verify the validity of the simulation. The WSCC 9-bus and IEEE 30-bus systems are performed to validate the suggested methodology. Section V discusses the main findings from this research and describes the effect of adding shunt reactor on the performance of the simulated systems. Finally, Section VI concludes the paper.

## II. FERRANTI EFFECT PHENOMENA

Under the Ferranti effect, no-load and light load conditions make the receiving end voltage greater than the sending end voltage due to the capacitive effect of the transmission line. If the receiving end voltage exceeds the limit, it damages the connected load, which is why reducing the Ferranti effect is essential [14], [15].

The transmission lines can be classified as short, medium, and long. Among these classifications, the long transmission line is composed of the highest capacitance and inductance distributed along the length. Therefore, the Ferranti effect is significant in the case of the long-length transmission lines. This is caused by an extremely high charging current in the line. The Ferranti effect is the name given to this event. Due to the capacitive effect of the line, a charged open
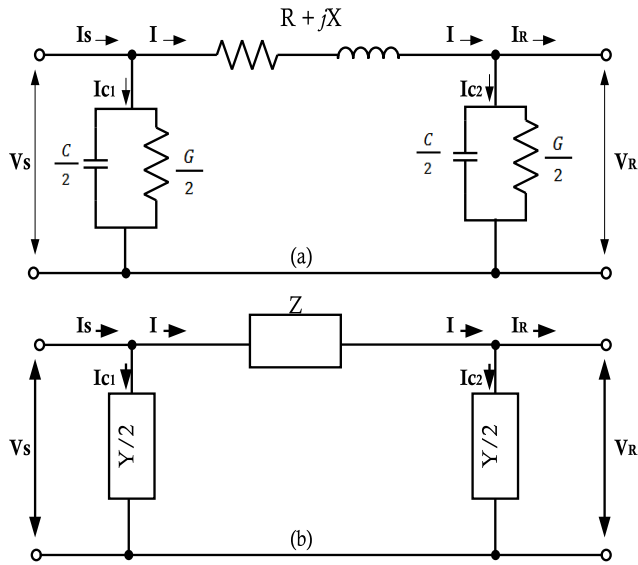
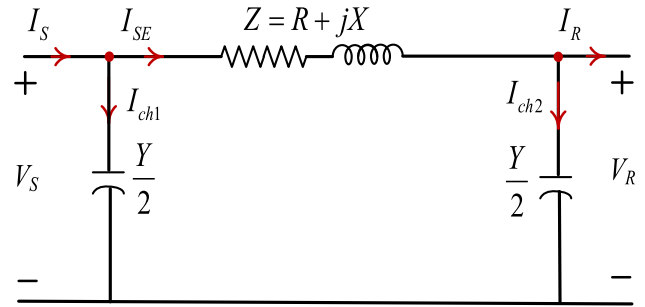FIGURE 1. Nominal-$\pi$ circuit: (a) actual circuit and (b) its equivalent lumped circuit.



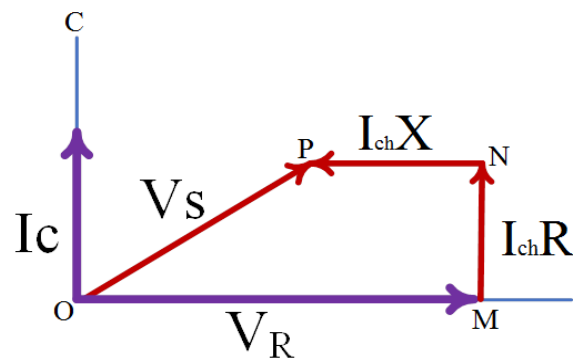FIGURE 2. Nominal-$\pi$ of transmission line under no-load condition.



FIGURE 3. Phasor diagram of Ferranti effect in transmission lines.



FIGURE 4. Voltage profile of an uncompensated line with fixed sending end voltage.

circuit line draws a considerable amount of current. This is especially true in high-voltage, long-distance transmission lines [14] [23]. In short lines, the capacitance (and charging current) is insignificant, but it is substantial in medium length lines and significant in long lines. As a result, this phenomenon only happens in medium and long lines [15].

The Ferranti effect is mainly caused by the effect of inductance and capacitance at light load conditions on the receiving end voltage of AC transmission lines [3], [23]. The shunt compensation and series compensation can be employed in transmission lines to reduce the Ferranti effect.

### A. TRANSMISSION LINE MODELS

Consider a nominal ï model of a long transmission line. The capacitor charging current through the distributed inductance of the transmission line creates a voltage drop across it (which is in-phase with the sending end voltage). The resultant receiving end voltage becomes greater than the sending end voltage. This phenomenon of overvoltage in a transmission line's receiving end at no load or light load conditions is called the Ferranti effect. Under the Ferranti effect, the reactive power generated is more than the reactive power absorbed, and this causes the voltage to rise in the receiving end.

For short transmission lines, capacitance and leakage resistance to the ground are typically ignored. Capacitance is ignored due to shorter lengths and lower voltages, while leakage resistance is ignored due to a relatively low leakage current compared to nominal current. However, as the line length and voltage increase, the model developed for short transmission lines produces inaccurate results. As a result, the impact of current leaking through the capacitance must be included for a more accurate approximation. As illustrated in Fig. 1, the shunt admittance is "lumped" at a few points
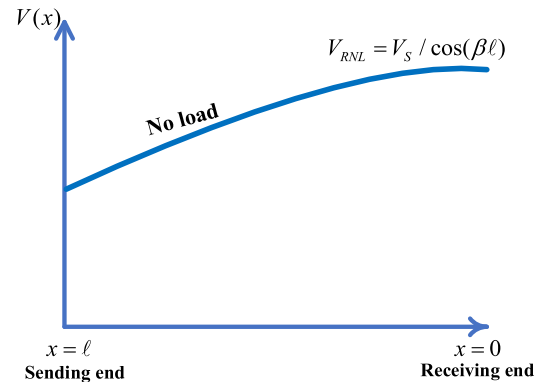
along the line and represented by creating a $\pi$ network [24]. Fig. 1(b) shows that the series parameters of the transmission line are lumped to form series impedance Z=R+j$\omega$L, and the shunt parameters are lumped to form shunt admittance Y=G+j$\omega$C.

On a per-phase basis, transmission lines are represented by an equivalent model [25]. It is convenient to represent a transmission line by the two-port network wherein sending end quantities (sending end voltage $V_s$ and current $I_s$) are given by receiving end quantities (receiving-end voltage $V_R$ and current $I_R$). In terms of the generalized circuit constants, the relation between the sending-end and receiving-end quantities is
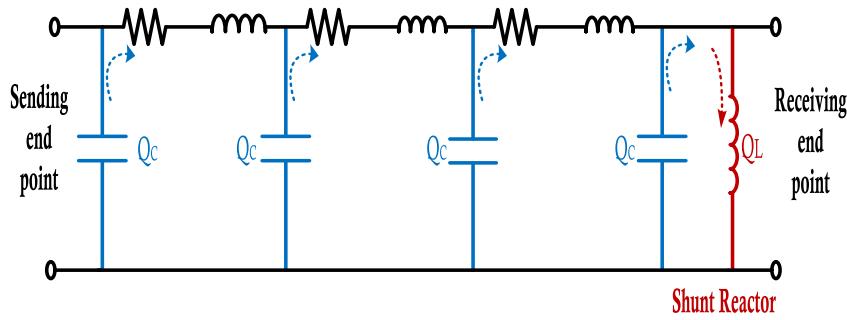
**FIGURE 5.** Reactive powers generated from capacitance are consumed by the shunt reactor.
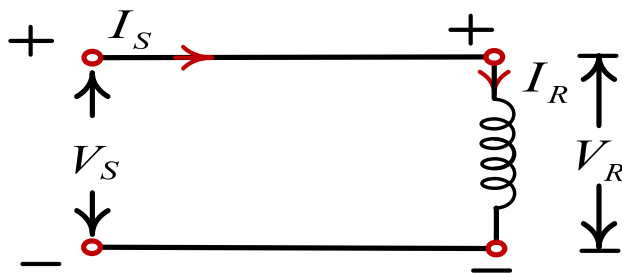


**FIGURE 6.** Shunt reactor compensation.



**FIGURE 7.** Voltage profile of an uncompensated and compensated line with fixed sending end voltage.

as follows [26]:

$$V_s = AV_R + BI_R \quad (1)$$
$$I_S = CV_R + DI_R \quad (2)$$

A long transmission line draws a lot of charging current. If the receiving end of such a line is open-circuited or extremely lightly loaded, the voltage at the receiving end may exceed the voltage at the transmitting end. This is known as the ferranti effect and is due to the charging current ($I_{ch}$) being in phase with the transmitting end voltage. As a result, both capacitance and inductance are required to produce this effect. As illustrated in Fig. 2, the line is represented by a nominal circuit with half of the total line capacitance concentrated at the receiving end. The phasor diagram of Fig. 3 illustrates the Ferranti effect.

OM represents the receiving end voltage, the current drawn by capacitance is assumed to be concentrated at the receiving end by OC, the resistance drop is represented by MN, the inductive reactance drop is represented by NP, and the sending end voltage is represented by OP, which is less than the receiving end voltage under no-load condition [15]. The voltage equation at the sending end is written as,

$$V_S = V_R + I_{ch}Z \quad (3)$$

For most high voltage transmission networks the R/X ratio is quite small [27]. Furthermore, the resistance drop MN is in quadrature with OM and NP. As a result, the resistance can be
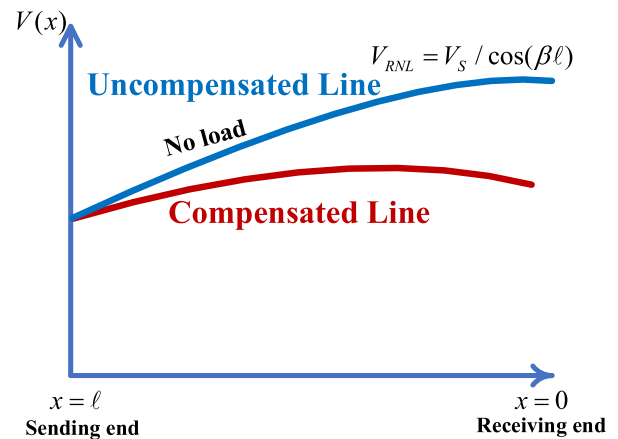
ignored when computing the Ferranti effect. Refer to (1) and under no-load condition ($I_R = 0$) the receiving end voltage is as follows:

$$V_R = \frac{V_S}{A} \quad (4)$$

For a nominal-π model the constant A defined as A= 1 + ZY/2, where Z=jωL and Y=jωC. Substituting for the product of Z and Y yields:

$$A = 1 - \frac{\omega^2 LC}{2} \quad (5)$$

Equation (5) indicates that as the length of the transmission line increases, the constant A is less than unity, and from (4) as the length of the transmission line increases, the voltage rise at the receiving end under no load condition will become larger [15], [19], [28]. Fig. 4 shows the voltage profile for an uncompensated transmission line with a fixed sending end voltage. The no-load voltage increases from $V_s = AV_{RNL}$ at the sending end to $V_{RNL}$ at the receiving end (where x = 0) [24]. Without some form of shunt compensation, maintaining voltages within reasonable limits becomes impossible for very long transmission lines [12].
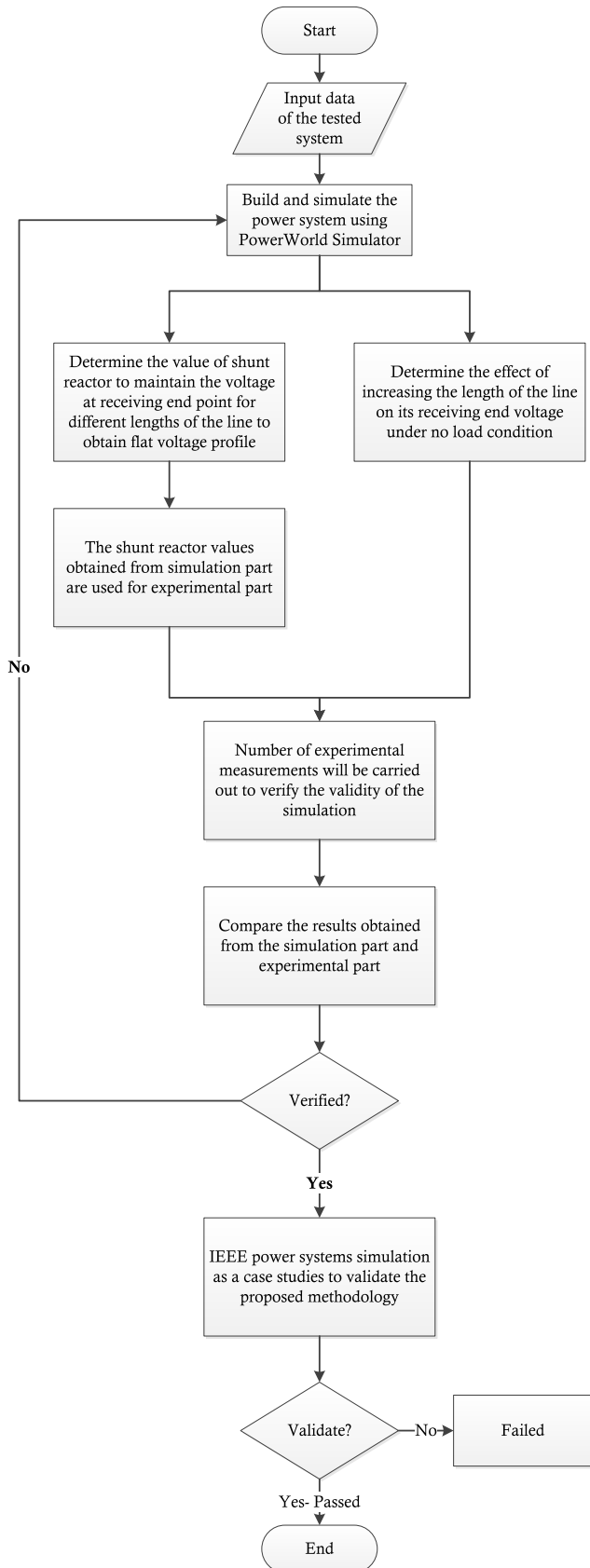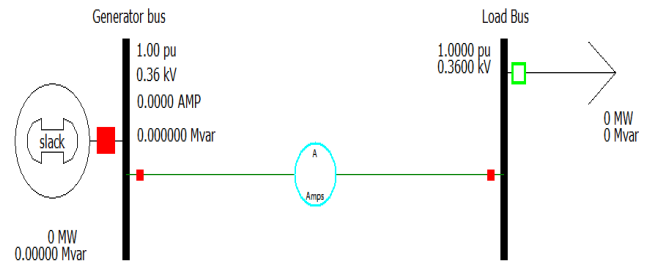
**FIGURE 9.** Single line diagram of the power system.

## B. SHUNT COMPENSATION

The line produces more reactive power than it consumes under light load or open line conditions; therefore, there is an excess of reactive power on the line, resulting in the receiving-end voltage being higher than the sending-end voltage. When the system is lightly loaded or open circuited, a device that absorbs reactive power must be added to the system to consume the excess reactive power.

A compensator mitigates the undesirable effects of the circuit parameters of a given line, shunt reactive compensation is used to adjust voltage magnitude, enhance voltage quality, and improve system stability. The shunt reactors used to minimize high voltages under light load or open line conditions, with the inductors absorbing reactive power and reducing overvoltages. Therefore, the reactive power generated by the shunt capacitance of the line are consumed by the shunt reactors connected in parallel with the line, as shown in Fig. 5 [29], [30], [31], [32].

The amount of reactor compensation needed to maintain a specified receiving end voltage on a transmission line can be determined as follows [25], [26], and [33]. Consider a reactor with a reactance of $X_{Lsh}$, which is connected to the receiving end of a long transmission line as illustrated in Fig. 6.

The receiving end current is given by:

$$I_R = \frac{V_R}{jX_{Lsh}} \qquad (6)$$

The voltage at a distance x from the receiving end is given by:

$$V(x) = \cos(\beta x) V_R + jZ_C \sin(\beta x) I_R \qquad (7)$$

Substituting for $I_R$ in (7) yields:

$$Vs = \left[\cos(\beta l) + \frac{Z_c \sin(\beta l)}{X_{lsh}}\right] V_R \qquad (8)$$

Equation (8) gets simplified as:

$$X_{lsh} = \frac{Z_c \sin(\beta l)}{(\frac{V_S}{V_R} - \cos(\beta l))} \qquad (9)$$

Equation (9) provides the value of the shunt reactor to be connected at the receiving end point [25], [33]. It is possible to deliver large amounts of power effectively with a flat voltage



**FIGURE 8.** Flowchart of the methodology.

**TABLE 1.** Simulation results for different lengths of the transmission line.

| Line length (km) | Sending end voltage (V) | Receiving end voltage (V) | Charging current (mA) | Sending end Reactive Power (Var) |
|---|---|---|---|---|
| 50 | 360 | 361.0 | 52.30 | -33.0 |
| 75 | 360 | 362.3 | 78.60 | -49.0 |
| 100 | 360 | 364.1 | 105.2 | -66.0 |
| 200 | 360 | 376.8 | 215.3 | -134 |
| 250 | 360 | 386.7 | 273.8 | -171 |
| 300 | 360 | 392.2 | 335.7 | -209 |
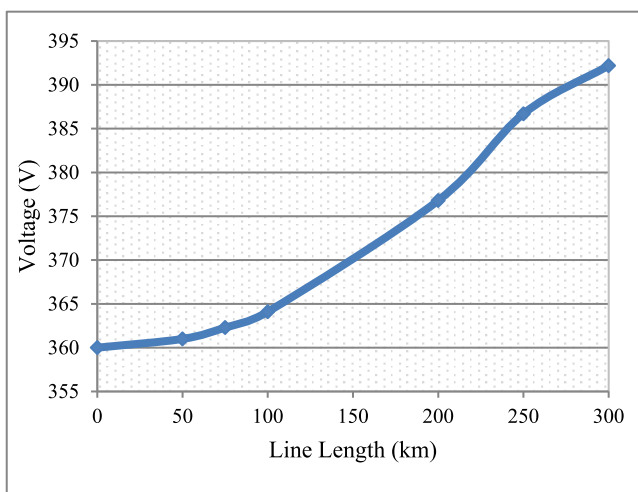


**FIGURE 10.** Voltage profile of an uncompensated transmission line with fixed sending end voltage.



**FIGURE 11.** Single line diagram of the power system with a shunt reactor at the receiving end point.

**TABLE 2.** Simulation results for the medium and long length transmission lines with shunt reactor compensation to obtain flat voltage profile.

| Length (km) | Receiving end voltage (V) | Receiving end Reactive power (Var) | Inductor value (mH) |
|---|---|---|---|
| 200 | 360 | 65.29 | 6322 |
| 250 | 360 | 81.74 | 5049 |
| 300 | 360 | 98.29 | 4197 |

**TABLE 3.** Inductor values for each step in the modules IL-2/EV and RL-2k/EV.

| Module IL-2/EV | | Module RL-2k/EV | |
|---|---|---|---|
| Step | Inductor value (mH) | Step | Inductor value (mH) |
| A | 2300 | A | 1400 |
| B | 1150 | B | 700 |
| C | 575 | C | 400 |

**TABLE 4.** Inductor values to obtain flat voltage profile.

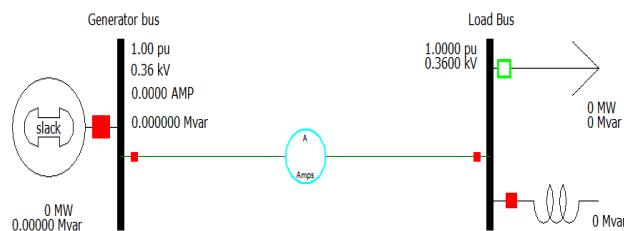| Length (km) | Inductor value (mH) |
|---|---|
| 200 | 6400 |
| 250 | 5100 |
| 300 | 4150 |

profile for shunt compensation of long transmission lines. Proper compensation should be provided in proper quantity at appropriate places to achieve the desired voltage control [34]. The voltage profile of an uncompensated and compensated line with a fixed sending voltage is shown in Fig. 7 [26].

## III. METHODOLOGY

Fig. 8 shows the flow chart that describes the methodology throughout the process used in this study. It consists of experimental tests and software simulations. The methodology of this study is divided into three stages.

In the first stage, simple two-bus power system was simulated using PowerWorld simulator to accomplish the following purposes:

- Investigate the effect of increasing the transmission line length on the receiving end voltage under no-load condition. The idea behind increasing the length of the line is to simulate each type of transmission line, including short, medium, and long lines, and analyze how they affect the receiving end voltage of the line under no load condition.
- Determine the shunt reactor value required to obtain flat voltage profile and mitigate Ferrante effect.

In the second stage, experimental tests conducted in the laboratory on the two-bus power system to verify the software results and realize that PowerWorld simulator can be used to estimate the value of the shunt reactor required to mitigate Ferranti effect.

The following steps used to carry out the previous stages:

1. The data needed to model the simple two-bus power system that is conducted in the laboratory is prepared.
2. The system is built using PowerWorld simulator to set model parameters for each component and circuit.
3. The effect of increasing the length of the transmission line on its receiving end voltage under no-load condition is obtained using the simulator.
4. The shunt reactor values required to maintain the receiving end voltage to obtain flat voltage profile in case of medium and long lengths transmission line are determined.

**TABLE 5.** Simulation results for the medium and long length transmission lines with shunt compensation.

| Length: 200-km | | | | |
|---|---|---|---|---|
| Inductance (mH) | Sending end voltage (V) | Receiving end voltage (V) | Charging current (mA) | Sending end Reactive Power (Var) |
| 6400 | 360 | 360.2 | 107 | -66.7 |
| Length: 250-km | | | | |
| Inductance (mH) | Sending end voltage (V) | Receiving end voltage (V) | Charging current (mA) | Sending end Reactive Power (Var) |
| 5100 | 360 | 360.3 | 134.4 | -83.77 |
| Length: 300-km | | | | |
| Inductance (mH) | Sending end voltage (V) | Receiving end voltage (V) | Charging current (mA) | Sending end Reactive Power (Var) |
| 4150 | 360 | 359.6 | 159.2 | -99.21 |
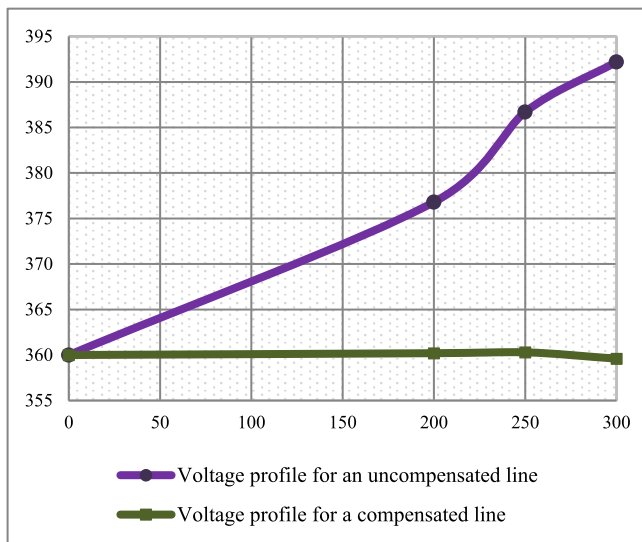


**FIGURE 12.** Voltage profiles of an uncompensated and compensated transmission line with fixed sending end voltage.

5. The obtained shunt reactor values in step 4 are used in the experimental part.
6. The results obtained from the experimental and simulation parts are compared to verify the software results.

In the last stage, the WSCC 9-bus and IEEE 30-bus systems are simulated to validate the proposed methodology.

## IV. FERRANTI EFFECT SIMULATION

To study the effect of increasing the length of transmission line on the receiving end voltage and estimate the shunt reactor value required to maintain the voltage at the receiving end point, a simple two-bus power system is used as a case study. First, this system is simulated using PowerWorld simulator to determine the effect of increasing the line length on the receiving end voltage and to obtain the value of the shunt reactor needed to obtain flat voltage profile. This system is simulated to compare the results with experimental measure-

ments made for the same conditions. Shunt reactor values obtained from simulation results are used in the experiment part to verify the simulation validity.

After verifying the simulation validity, WSCC 9-bus and IEEE 30-bus systems are simulated to validate the proposed methodology.

### A. SIMPLE 2-BUS POWER SYSTEM SIMULATION

The single-line diagram of the system shown in Fig. 9 is built in PowerWorld simulator. This network consists of two buses, one source, one branch, and one load. The simulation allows changing transmission line parameters to obtain different lengths of the transmission line.

In order to determine the effect of increasing transmission line length on the receiving end voltage with fixed sending end voltage, different lengths of the transmission line have been simulated.

The first two cases represent a short-length transmission line of 50 and 75-km, the second two cases represent a medium-length transmission line of 100 and 200-km, and the last two cases represent a long-length transmission line of 250 and 300-km. The simulation results of the receiving end voltage, charging current, and line generated reactive power for each case are shown in Table 1.

According to the results in Table 1, it is shown that the receiving end voltage, charging current, and reactive power generated by the transmission line all increase as the transmission line's length increases with fixed sending end voltage. The voltage profile for an uncompensated transmission line with a fixed sending end voltage is shown in Fig. 10.

In case of medium and long length transmission lines, a shunt reactor has been added to maintain the voltage at the receiving end point. Fig. 11 shows the single-line diagram of the power system with a shunt reactor.

The reactive power consumed by the inductor to maintain the voltage profile is obtained from simulation results. Equation (10) is used to determine the size of the inductor in mH.

$$L = \left[ \frac{V_L^2 * 10}{Q_L * \pi} \right] \quad (10)$$

where $V_L$ represents the connected reactor bus voltage in (V) and $Q_L$ represents the reactive power absorbed by the reactor in (var).

To determine the shunt reactor value needed to obtain flat voltage profile, the reactive power consumed by the reactor to maintain the voltage profile is obtained from simulation results. Table 2 shows the simulation results for medium and long lengths transmission line with shunt reactor compensation to obtain flat voltage profile.

The inductors used in the lab are of two types: IL-2/EV and RL-2k/EV. The inductor values for each module are represented in Table 3.

The inductor values that should be installed at the receiving end point of the transmission line in order to obtain flat voltage profiles for different lengths of the transmission line

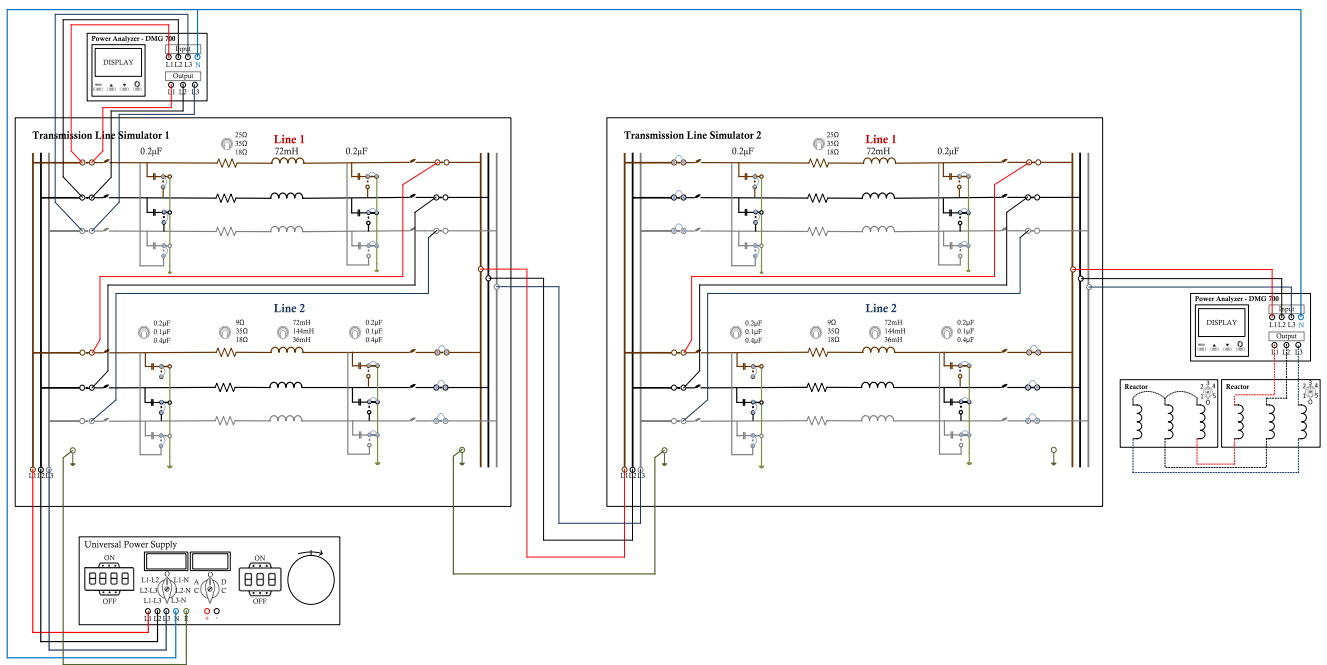**FIGURE 13.** Equipment used in the laboratory.



**FIGURE 14.** Connection between equipment used in the experiment.

are shown in Table 4. These were determined based on the inductor values from Tables 2 and 3.

The inductor values are chosen as same as that used in the lab, the receiving end voltage, charging current and sending end reactive power have been measured and tabulated as shown in Table 5.

The above cases have been simulated in order to compare them to experimental measurements made for the same conditions. Fig. 12 shows the voltage profile of an uncompensated and compensated transmission line with a fixed sending end voltage for transmission lines of 200, 250, and 300 km length.

## B. SIMPLE 2-BUS POWER SYSTEM EXPERIMENTAL VALIDATION

A number of experimental measurements have been carried out to study Ferranti effect of the transmission line and to verify the validity of the simulation. The experiment equipment, which includes a variable three-phase power supply, transmission line simulators, and a digital power analyzer, is shown in Fig. 13.

Transmission line simulator consists of two lines with the possibility of varying their parameters. Table 6 represents the line 1 and line 2 specifications of the transmission line simulator.

**TABLE 6.** Specifications of the Transmission Line Simulator used in the lab.

| Parameters | Line 1 | Line 2 |
|---|---|---|
| Rated voltage | 380-V | 380-V |
| Rated current | 1-A | 1-A |
| Rated Power | 657.4-VA | 657.4-VA |
| Equivalent resistance | 18-25-35-Ω | 8.9-25-35-Ω |
| Equivalent inductance | 72-mH | 36-72-144-mH |
| Equivalent Capacitance | 2x0.2-µF | 2x0.1-0.2-0.4-µF |
| Length | 50-km | 25-50-100-km |

**TABLE 7.** Experimental results for the no-load transmission line at different lengths.

| Line length (km) | Sending end voltage (V) | Receiving end voltage (V) | Charging current (mA) | Sending end Reactive Power (Var) |
|---|---|---|---|---|
| 50 | 360 | 360.5 | 55.0 | -33.50 |
| 75 | 360 | 361.6 | 83.0 | -50.80 |
| 100 | 360 | 363.5 | 108 | -68.20 |
| 200 | 360 | 370.1 | 218 | -135.0 |
| 250 | 360 | 382.0 | 278 | -173.3 |
| 300 | 360 | 397.0 | 334 | -210.0 |

The experiment has been carried out with transmission line under no load condition at different lengths after appropriate connection between the experiment equipment as shown in the Fig. 14.

The value of the sending end voltage, receiving end voltage, charging current and sending end reactive power have been measured by the three-phase power analyzer and tabulated as shown in Table 7.

From the results obtained in Table 7, it is observed that the increasing in the receiving end voltage for short transmission lines is negligible but considerable in medium length lines and appreciable in long lines. Fig. 15 shows the voltage profile for an uncompensated transmission line with fixed sending end voltage.

The sending end voltage, receiving end voltage, charging current and sending end reactive power have been measured by the three-phase power analyzer after the inductors have been connected at the transmission line's receiving end point. The experiment was carried with a transmission line simulator under no load condition with shunt reactor compensation at different lengths, the measured quantities are tabulated as shown in Table 8.

Fig. 16 shows the voltage profiles for an uncompensated and compensated transmission line in case of 200, 250 and 300-km length line with fixed sending end voltage.

The results of both hardware and software of the receiving end voltage of the transmission line have been compared in terms of percentage error in order to determine the accuracy and effectiveness of the simulation model, as shown in Tables 9 and 10. Hardware and software results for the receiving end voltage without compensation are shown in
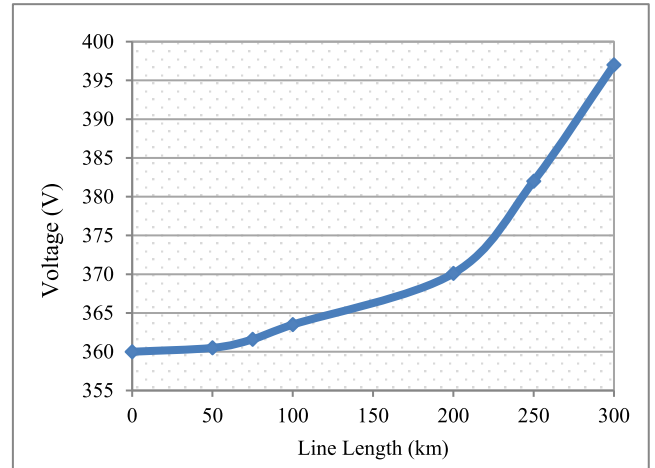


**FIGURE 15.** Voltage profile of an uncompensated transmission line with fixed sending end voltage.

**TABLE 8.** Experimental results of the medium and long length transmission lines with shunt compensation.

| Length: 200-km | | | | |
|---|---|---|---|---|
| Inductance (mH) | Sending end voltage (V) | Receiving end voltage (V) | Charging current (mA) | Sending end Reactive Power (Var) |
| 6400 | 360 | 358.6 | 57 | -85.5 |
| Length: 250-km | | | | |
| Inductance (mH) | Sending end voltage (V) | Receiving end voltage (V) | Charging current (mA) | Sending end Reactive Power (Var) |
| 5100 | 360 | 360 | 78 | -109.6 |
| Length: 300-km | | | | |
| Inductance (mH) | Sending end voltage (V) | Receiving end voltage (V) | Charging current (mA) | Sending end Reactive Power (Var) |
| 4150 | 360 | 363 | 101 | -133.6 |

**TABLE 9.** Receiving end voltage determined by experiment and simulation and the corresponding error without compensation condition.

| Length (km) | Receiving end voltage without compensation (V) | | |
|---|---|---|---|
| | Experiment | Simulation | Error (%) |
| 50 | 360.5 | 361.0 | 0.139 |
| 75 | 361.6 | 362.3 | 0.194 |
| 100 | 363.5 | 364.1 | 0.165 |
| 200 | 370.1 | 376.8 | 1.810 |
| 250 | 382.0 | 386.7 | 1.230 |
| 300 | 397.0 | 392.2 | 1.209 |

Table 9, whereas results for the receiving end voltage with compensation are shown in Table 10. The results show that the average relative error for both conditions is less than 1%, indicating that the simulation's validity has been established.
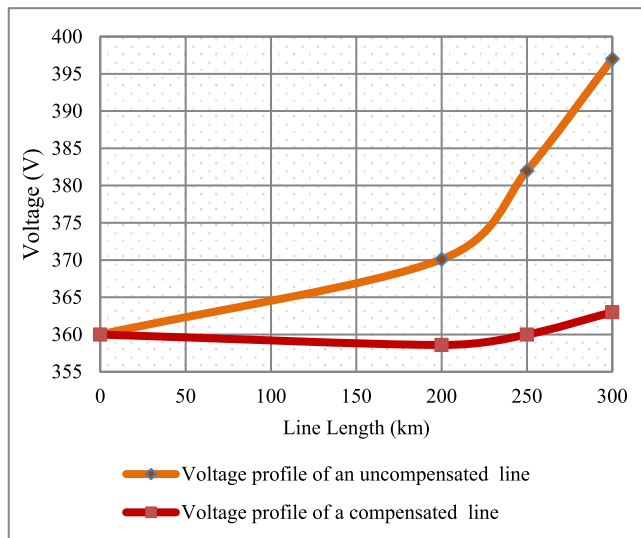
**FIGURE 16.** Voltage profiles of an uncompensated and compensated transmission line with fixed sending end voltage.

**TABLE 10.** Receiving end voltage determined by experiment and simulation and the corresponding error with compensation condition.

| Length (km) | Receiving end voltage with compensation (V) | | |
|---|---|---|---|
| | Experiment | Simulation | Error (%) |
| 200 | 358.6 | 360.2 | 0.446 |
| 250 | 360.0 | 360.3 | 0.083 |
| 300 | 363.0 | 359.6 | 0.937 |

**TABLE 11.** Main characteristics of the WSCC 9-bus and 30-bus systems.

| Item | WSCC 9-bus system | IEEE 30-bus system |
|---|---|---|
| Number of buses | 9 | 30 |
| Number of generators | 3 | 6 |
| Number of branches | 9 | 37 |
| Number of loads | 3 | 21 |
| Total connected loads | 335.34MVA | 310.23MVA |

## C. IEEE BUS SYSTEMS SIMULATION

Many studies on the IEEE bus systems have been conducted, covering a wide range of topics. In this section we present a number of such studies that are relevant to this work. The WSCC 9-bus and standard IEEE 30-bus systems are carried out as case studies. The core features of the two test systems are specified in Table 11. The data of the test systems have been obtained from [35] and [36].
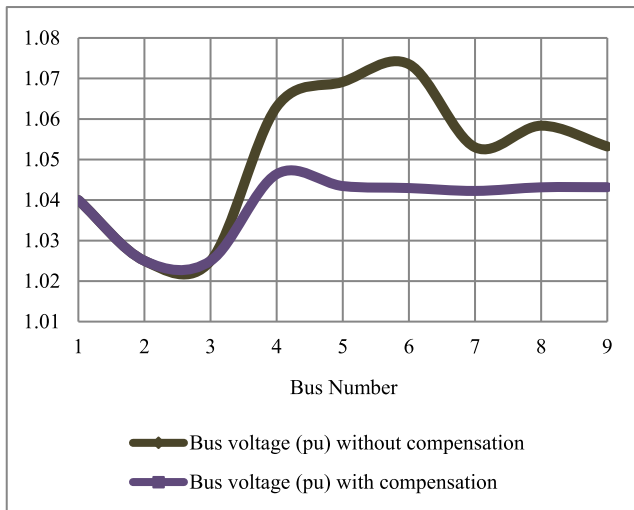
The aim is to study Ferranti effect and find the shunt reactor value required to maintain the bus voltage within specified limits ($0.95 \leq V_{bus} \leq 1.05$). To demonstrate the efficiency of the proposed method, two cases have been simulated using PowerWorld simulator. In the case I, the loads are reduced to 90 percent of the system MVA load, resulting in a lightly

**TABLE 12.** Simulation results for 90% load reduction condition.

| Test system | Total connected load in MVA | Buses with voltage higher than the upper limit | | System generated reactive power in Mvar |
|---|---|---|---|---|
| | | Bus number | Bus voltage in PU | |
| **WSCC 9-bus system** | 33.534 | 4 | 1.06300 | 148.2342 |
| | | 5 | 1.06915 | |
| | | 6 | 1.07352 | |
| | | 7 | 1.05301 | |
| | | 8 | 1.05835 | |
| | | 9 | 1.05322 | |
| | Total MW Losses | 0.1766 | | |
| | Highest line Mvar generated | Line 9-6 | 26.3 Mvar | |
| | | Line 7-5 | 22.7 Mvar | |
| | | Line 7-8 | 20.9 Mvar | |
| **IEEE 30-bus system** | 31.023 | 3 | 1.05545 | 32.9174 |
| | | 4 | 1.05327 | |
| | | 9 | 1.07392 | |
| | | 10 | 1.08226 | |
| | | 12 | 1.06888 | |
| | | 14 | 1.06941 | |
| | | 15 | 1.07075 | |
| | | 16 | 1.07378 | |
| | | 17 | 1.07917 | |
| | | 18 | 1.07363 | |
| | | 19 | 1.07564 | |
| | | 20 | 1.07721 | |
| | | 21 | 1.08076 | |
| | | 22 | 1.08070 | |
| | | 23 | 1.07355 | |
| | | 24 | 1.07809 | |
| | | 25 | 1.06743 | |
| | | 26 | 1.06578 | |
| | | 27 | 1.06154 | |
| | | 28 | 1.05155 | |
| | | 29 | 1.05971 | |
| | | 30 | 1.05865 | |
| | Total MW Losses | 0.7560 | | |
| | Highest lines Mvar generated | Line 5-7 | 39.3 Mvar | |
| | | Line 2-4 | 12.5 Mvar | |
| | | Line 2-6 | 9.70 Mvar | |
| | | Line 11-9 | 8.50 Mvar | |
| | | Line 6-28 | 6.40 Mvar | |
| | | Line 16-17 | 6.10 Mvar | |
| | | Line 8-28 | 5.70 Mvar | |
| | | Line 12-16 | 5.00 Mvar | |
| | | Line 12-15 | 4.50 Mvar | |
| | | Line 19-20 | 3.90 Mvar | |
| | | Line 23-24 | 3.60 Mvar | |
| | | Line 12-13 | 3.40 Mvar | |
| | | Line 15-23 | 3.30 Mvar | |
| | | Line 18-19 | 3.20 Mvar | |
| | | Line 15-18 | 3.00 Mvar | |
| | | Line 14-15 | 1.30 Mvar | |
| | | Line 12-14 | 1.00 Mvar | |
| | | Line 12-16 | 6.60 Mvar | |
| | | Line 12-15 | 4.50 Mvar | |
| | | Line 23-24 | 4.50 Mvar | |
| | | Line 15-23 | 4.40 Mvar | |
| | | Line 19-20 | 3.80 Mvar | |
| | | Line 18-19 | 3.80 Mvar | |
| | | Line 15-18 | 3.80 Mvar | |
| | | Line 11-9 | 3.60 Mvar | |
| | | Line 14-15 | 1.60 Mvar | |
| | | Line 12-14 | 1.60 Mvar | |

**TABLE 13.** Reactor size, location and system MW losses in the case of a 90% load reduction compensation.

| Test system | Reactor location | Reactor rating in Mvar | System Losses in MW |
|---|---|---|---|
| WSCC 9-bus system | Bus 5 | 22.864 | 0.0330 |
| | Bus 6 | 27.194 | |
| | Bus 8 | 13.058 | |
| IEEE 30-bus system | Bus 4 | 21.269 | 0.6910 |
| | Bus 6 | 11.596 | |
| | Bus 7 | 14.369 | |
| | Bus 11 | 18.469 | |
| | Bus 15 | 9.7180 | |
| | Bus 16 | 2.1790 | |
| | Bus 17 | 4.3630 | |
| | Bus 20 | 2.1700 | |
| | Bus 28 | 1.0560 | |



**FIGURE 17.** Voltage profiles of the WSCC 9-bus system for case I.

**TABLE 14.** Simulation results for 100% load reduction condition.

| Test system | Total connected load in MVA | Buses with voltage higher than the upper limit | | System generated reactive power in Mvar |
|---|---|---|---|---|
| | | Bus number | Bus voltage in PU | |
| WSCC 9-bus system | 0 | 4 | 1.06607 | 148.7638 |
| | | 5 | 1.07523 | |
| | | 6 | 1.07892 | |
| | | 7 | 1.05520 | |
| | | 8 | 1.06203 | |
| | | 9 | 1.05483 | |
| | Total MW Losses | 0.1938 | | |
| | Highest line Mvar generated | Line 9-6 | 28.6 Mvar | |
| | | Line 7-5 | 25.9 Mvar | |
| | | Line 7-8 | 25.0 Mvar | |
| IEEE 30-bus system | 0 | 3 | 1.05889 | 33.5422 |
| | | 4 | 1.05764 | |
| | | 6 | 1.05559 | |
| | | 9 | 1.07852 | |
| | | 10 | 1.08881 | |
| | | 12 | 1.07271 | |
| | | 14 | 1.07490 | |
| | | 15 | 1.07688 | |
| | | 16 | 1.07948 | |
| | | 17 | 1.08594 | |
| | | 18 | 1.08106 | |
| | | 19 | 1.08353 | |
| | | 20 | 1.08484 | |
| | | 21 | 1.08850 | |
| | | 22 | 1.08841 | |
| | | 23 | 1.08121 | |
| | | 24 | 1.08700 | |
| | | 25 | 1.07628 | |
| | | 26 | 1.07628 | |
| | | 27 | 1.06955 | |
| | | 28 | 1.05793 | |
| | | 29 | 1.06955 | |
| | | 30 | 1.06955 | |
| | Total MW Losses | 0.6799 | | |
| | Highest lines Mvar generated | Line 5-7 | 43.1 Mvar | |
| | | Line 2-4 | 15.4 Mvar | |
| | | Line 2-6 | 13.0 Mvar | |
| | | Line 6-28 | 8.00 Mvar | |
| | | Line 8-28 | 7.10 Mvar | |
| | | Line 16-17 | 7.10 Mvar | |

loaded condition. Case II represents the worst-case scenario, in which all bus loads are reduced to zero, resulting in a no-load condition.

### 1) CASE I: 90% LOAD REDUCTION CONDITION

After reducing the overall load by 90% of the system MVA and running the load flow simulation for all test systems, the bus voltage, total MW losses, and lines Mvar generated results have been obtained. The buses with voltages higher than the upper limit and the lines with the highest Mvar generated are identified, and the systems' generated reactive power is specified as shown in Table 12.

It is observed from results in Table 12 that many of bus voltages are shown to be higher than the upper limit. This is dangerous to the power system because it affects equipment and load operations, system instability, and poor power quality, efficiency, and insulation failures, risky to Personnel and causing losses. The system requires inductive compensation to mitigate this situation. The shunt reactor's location is deter-mined by the maximum line Mvar. The size and location of the reactors that are installed to reduce this

effect and the new system losses after adding the shunt reactors are shown in Table 13.

It is observed from results in Table 12 that many of bus voltages are shown to be higher than the upper limit. This is dangerous to the power system because it affects equipment and load operations, system instability, and poor power quality, efficiency, and insulation failures, risky to Personnel and causing losses. The system requires inductive compensation
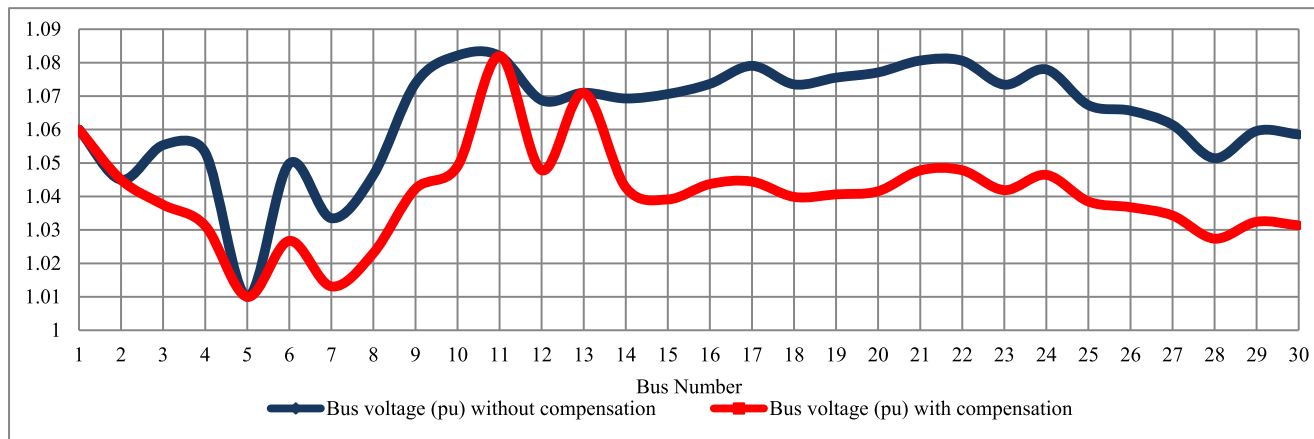
**FIGURE 18.** Voltage profiles of the IEEE 30-bus system for case I.

**TABLE 15.** Reactor size, location and system mw losses in the case of a 100% load reduction compensation.

| Test system | Reactor location | Reactor rating in Mvar | System Losses in MW |
|---|---|---|---|
| WSCC 9-bus system | Bus 5 | 27.305 | 0.0037 |
| | Bus 6 | 30.528 | |
| | Bus 8 | 16.341 | |
| IEEE 30-bus system | Bus 4 | 23.485 | 0.6382 |
| | Bus 6 | 12.723 | |
| | Bus 7 | 12.402 | |
| | Bus 9 | 17.435 | |
| | Bus 15 | 5.2390 | |
| | Bus 16 | 1.0960 | |
| | Bus 17 | 3.3790 | |
| | Bus 18 | 1.0770 | |
| | Bus 19 | 1.0740 | |
| | Bus 20 | 6.4450 | |
| | Bus 23 | 2.1700 | |
| | Bus 24 | 2.1910 | |
| | Bus 28 | 1.0630 | |



**FIGURE 19.** Voltage profiles of the WSCC 9-bus system for case II.

to mitigate this situation. The shunt reactor's location is determined by the maximum line Mvar. The size and location of the reactors that is installed to reduce this effect and the new system losses after adding the shunt reactors are shown in Table 13.

After the shunt reactors have been added to both test systems, it was found that the systems' MW losses had been decreased and the bus voltages had returned to being within the allowed limit. The size of the reactors is determined by PowerWorld simulator. The voltage profiles of the two test systems are shown in Fig. 17 and 18 for this case. All bus voltages are shown to be within the acceptable ranges.

### 2) CASE II: 100% LOAD REDUCTION CONDITION
In this case, the loads on all buses have been reduced to zero, a no load condition has been introduced, and the load flow simulation is running for all test systems. Similarly as
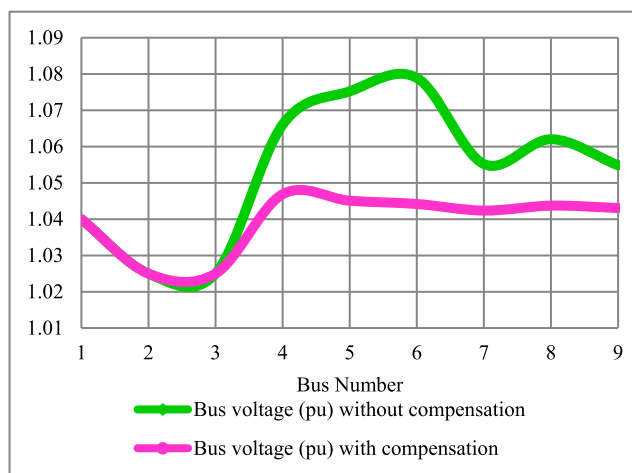
in the previous case, the bus voltage, total MW losses, and lines Mvar generated results have been obtained. The buses with voltages higher than the upper limit and the lines with the highest Mvar generated are identified, and the systems' generated reactive power is specified as shown in Table 14.

Because there is no longer any power being absorbed by the load, the reactive power generated from lines increases, causing the receiving end bus voltage to increase. The rise in the bus voltages has been larger than it was under the previous condition.

The size and location of the shunt reactors that have been used to maintain the bus voltages to be within limits and to reduce system MW losses and the new system losses after adding the shunt reactors are shown in Table 15.

It is shown that from the results obtained in Tables 13 and 15 the value of the shunt reactor required for compensation in the no load condition is greater than that in the light load condition.

Adding shunt reactors to mitigate the Ferranti effect will decrease the bus voltages to be within permissible limits and
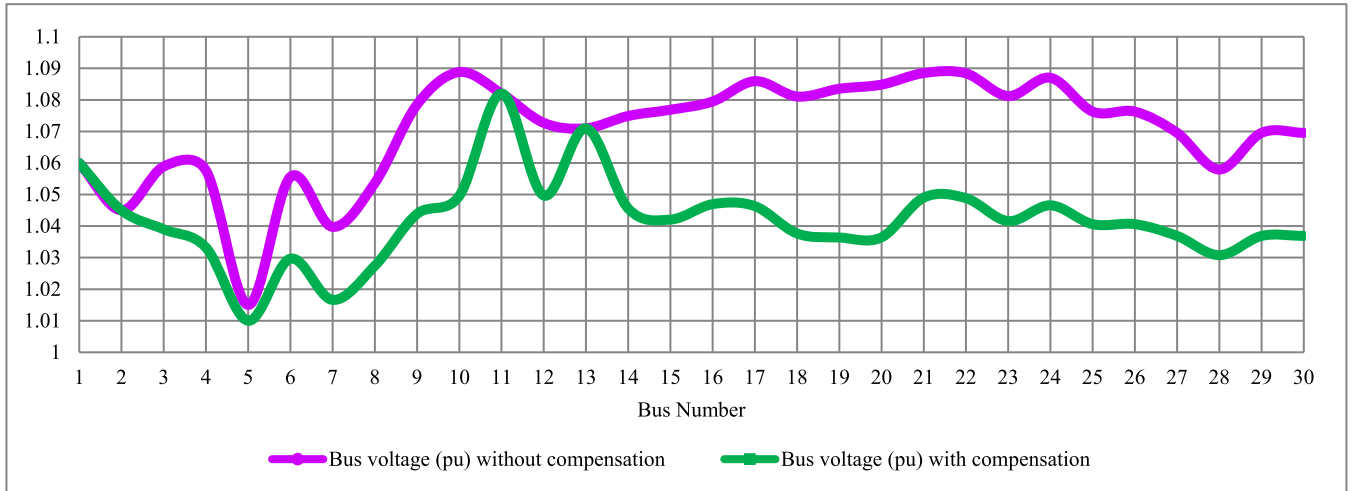
**FIGURE 20.** Voltage profiles of the IEEE 30-bus system for case II.

reduce system MW losses, the location of the shunt reactors is determined by the maximum line Mvar and the value of these reactors can be estimated by using PowerWorld simulator. The voltage profiles of the two test systems are shown in Fig. 19 and 20 for this case. All bus voltages are shown to be within the permissible limits.

## V. DISCUSSION

The main aim of this study was to estimate the value of the shunt reactor required to maintain the bus voltage in different cases. Using PowerWorld simulator, a simple two-bus system was modeled and simulated. Then, experiments were carried out on the same two-bus power system to compare the simulation and experimental results and to verify the suggested methodology. Case studies involving the

WSCC 9-bus and IEEE 30-bus systems were used to validate the proposed methodology.

The main findings from this study can be summarized as follows:

1. Under no-load condition, the increasing in the receiving end voltage for short transmission lines was negligible but considerable in medium length lines and appreciable in long lines.
2. PowerWorld simulator was effectively used to determine the required value of the shunt reactor to obtain flat voltage profile.
3. The simulation's validity was established by comparing the results of both hardware and software of the receiving end voltage.
4. The Ferranti effect was investigated in WSCC 9-bus and IEEE 30-bus systems for two cases, and the values of the shunt reactors required to maintain the bus voltage within specified limits ($0.95 \leq Vbus \leq 1.05$) were obtained.

5. The shunt reactor's location was determined by the maximum line Mvar, and the size of the reactors was determined by the simulator.

The following sections describe the effect of adding shunt reactor on the performance of the simulated systems.

### A. EFFECT ON THE VOLTAGE PROFILE AND VOLTAGE STABILITY

The bus voltage in the previous simulations should be kept in the 0.95-pu and 1.05-pu range. It was demonstrated that most bus voltages exceed the allowed maximum voltage level in the simulated cases without shunt compensation.

The primary cause of voltage instability is the unbalanced supply and demand for reactive power. According to our simulation studies, the amount of reactive power generated by the lines was significantly larger than the amount of reactive power required, which raised the voltage. Shunt reactors provided voltage stability since they maintain the voltage within the desired limits, as demonstrated by the results of the tested systems and shown in Fig. 17, 18, 19, and 20.

### B. EFFECT ON THE LINE LOADABILITY AND TRANSMISSION LOSSES

he loading of an open-line or lightly loaded transmission line is due to the charging current generated from transmission lines. It can be seen that in case the reactor is in service, most lines loadability is reduced which improved line energy efficiency. Fig. 21 shows the lines' loadability in each case, both before and after the reactors are added.

According to [37], it is desirable to install the shunt reactors in the middle of the line because reactive current would flow towards the reactor from both sides and only half of the charging current would be flowing at the points that are the most loaded. In the previous simulations, the shunt reactors were assumed to be connected to buses. As a result, some
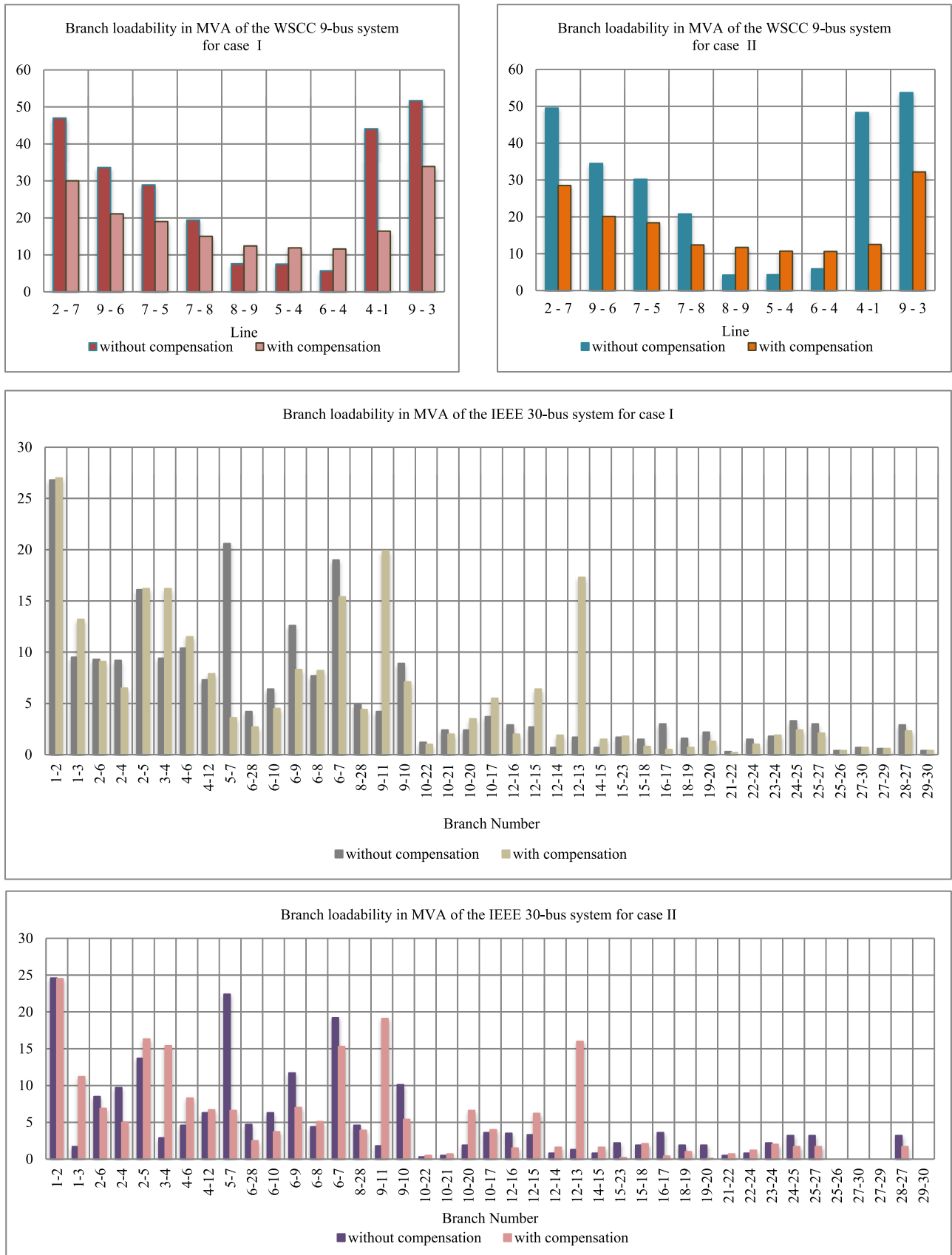
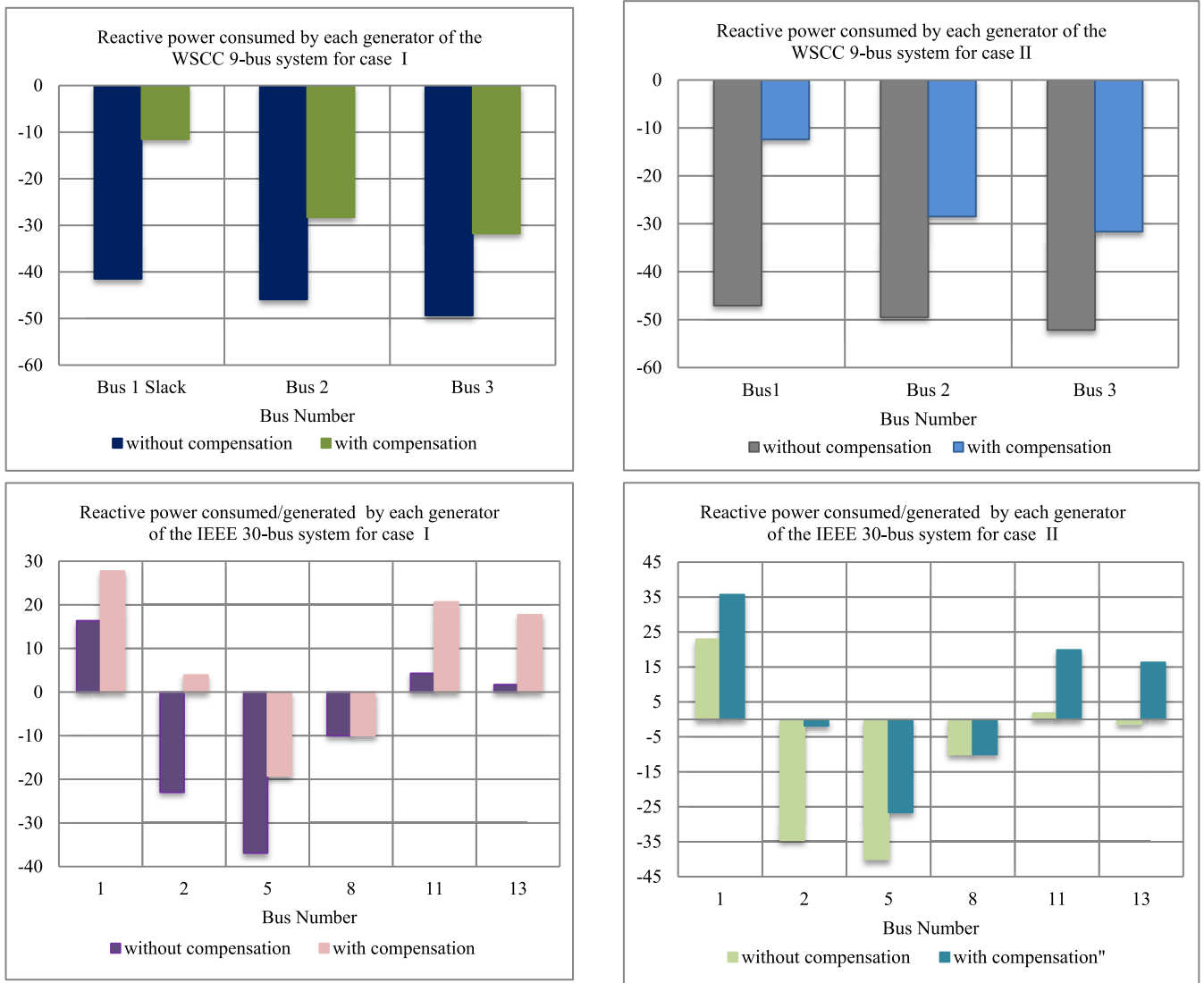**FIGURE 21.** Branch loadability for each of the simulated systems.

**FIGURE 22.** Reactive power consumed/generated by the generators for each of the simulated systems.

of the line's load capacity was increased. The transmission losses decreased after the shunt reactors were added because the reactive power was delivered locally and did not have to travel farther through the system resistances. Tables 13 and 15 present the value of the system losses for each of the simulated cases.

### C. EFFECT ON THE GENERATORS

Under no-load condition, the synchronous generators connected to a certain uncompensated transmission line were operated in the under-excited mode. Fig. 22 shows the reactive power absorbed/generated by the generators in each case. It was observed that the reactive power absorption reduced, thus moving the operating point of the generators to a more stable point in within the capability region. As synchrouns generator's reactive power consumption rises, their angular displacement also increases. Thus, the transmission angle

increases and raises the chance that the power system's transient stability may be lost. In each of the previous simulated cases, Fig. 23 illustrates the bus angle for each bus of the WSCC 9-bus and 30-bus systems.

### VI. CONCLUSION

This paper proposes an approach for estimating the shunt reactor value needed to maintain the voltage at the receiving end point of the transmission line under no-load and light load conditions. Under these conditions, the PowerWorld simulator has been used to determine the effect of increasing the length of the transmission line on its receiving end voltage and to estimate the value of the shunt reactor to mitigate the Ferranti effect. Case studies on both simulation and experimental tests were used to evaluate the efficiency of the proposed methodology. The proposed method succeeded in obtaining the shunt reactor value needed to maintain the
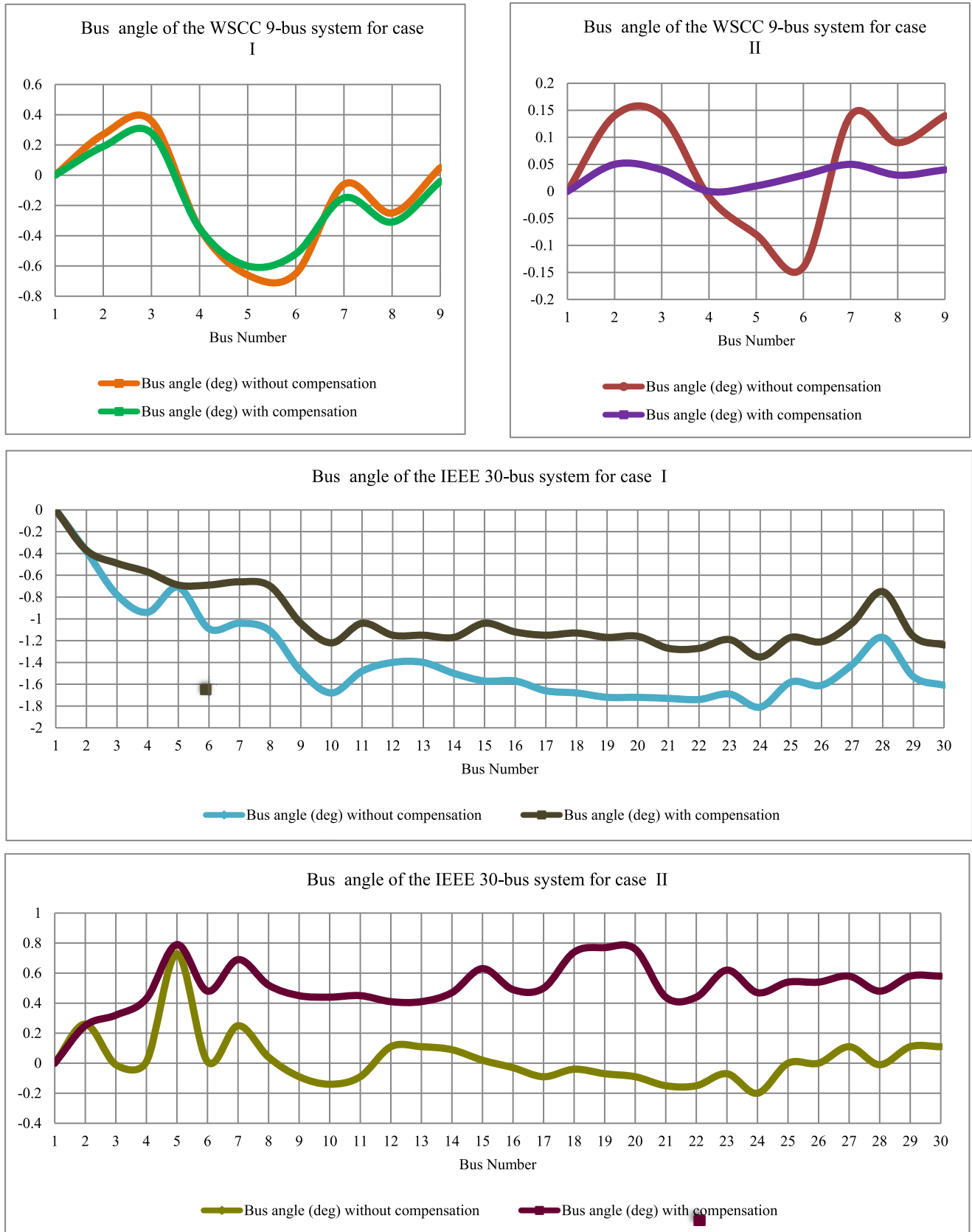
**FIGURE 23.** Bus angle value for each of the simulated systems.

bus voltages and mitigating Ferranti effect. In the case of a two-bus system and for the 250-km case study, the reactor value obtained from the simulator was 5049-mH, which was required to obtain a flat voltage profile. The receiving end voltage was measured to be 360.3-V when this reactor value was used in the experiment, which verified the simulation's results. WSCC 9-bus and IEEE 30-bus systems were used to validate the proposed approach. The results demonstrated the effectiveness of the proposed approach in maintaining voltage stability, minimizing line loadability and transmission losses, and reducing synchronous generator angular displacement. In this study, the reactors have been assumed to be connected at load buses. In the future, it is advised to consider installing shunt reactors in the middle of lines to enhance system performance.

## ACKNOWLEDGMENT

## REFERENCES

[1] M. Ghassemi, "High surge impedance loading (HSIL) lines: A review identifying opportunities, challenges, and future research needs," *IEEE Trans. Power Del.*, vol. 34, no. 5, pp. 1909–1924, Oct. 2019.

[2] N. F. A. Rahman, "Performance comparison of overhead line under various load conditions," *Int. J. Simul., Syst., Sci. Technol.*, vol. 17, no. 41, pp. 1–4, Jan. 2016.

[3] Cadence System Analysis. *How to Reduce the Ferranti Effect in AC Transmission Lines*. Accessed: Jun. 10, 2022. [Online]. Available: https://resources.system-analysis.cadence.com/blog/msa2021-how-to-reduce-the-ferranti-effect-in-ac-transmission-lines

[4] I. O. Zaitsev and V. V. Kuchanskyy, "Corona discharge problem in extra high voltage transmission line," in *Systems, Decision and Control in Energy II*. Springer, 2021, pp. 3–30.

[5] E. Stracqualursi, R. Araneo, and S. Celozzi, "The corona phenomenon in overhead lines: Critical overview of most common and reliable available models," *Energies*, vol. 14, no. 20, p. 6612, Oct. 2021.

[6] V. N. Ogar, S. A. Bendor, and A. E. James, "Analysis of corona effect on transmission line," *Amer. J. Eng. Res.*, vol. 6, pp. 75–87, 2017.

[7] J. R. Gonzalez-Teodoro, V. Kindl, E. Romero-Cadaval, and R. Asensi, "Analysis of skin effect in single wire resistance by finite element methods," in *Proc. IEEE 14th Int. Conf. Compat., Power Electron. Power Eng. (CPE-POWERENG)*, vol. 1, Jul. 2020, pp. 19–23.

[8] A. Młot, M. Korkosz, P. Grodzki, and M. Łukaniszyn, "Analysis of the proximity and skin effects on copper loss in a stator core," *Arch. Electr. Eng.*, vol. 63, no. 2, pp. 211–225, Jun. 2014.

[9] L. Guizhen, G. Qingxin, and L. Zengrui, "Study of the proximity effect and the distribution parameters of multi-conductor transmission line," in *Proc. IEEE Int. Conf. Microw. Millim. Wave Technol. (ICMMT)*, vol. 2, Jun. 2016, pp. 868–870.

[10] T. Asada, Y. Baba, N. Nagaoka, A. Ametani, J. Mahseredjian, and K. Yamamoto, "A study on basic characteristics of the proximity effect on conductors," *IEEE Trans. Power Del.*, vol. 32, no. 4, pp. 1790–1799, Aug. 2017.

[11] S. G. Ankaliki, P. S. Vibhuti, M. S. Sureban, and S. P. Amminabhavi, "Performance analysis of unloaded long transmission line using transmission line hardware simulator," *i-Manager's J. Power Syst. Eng.*, vol. 9, no. 1, pp. 1–7, 2021.

[12] G. Chavan, S. Acharya, S. Bhattacharya, D. Das, and H. Inam, "Application of static synchronous series compensators in mitigating Ferranti effect," in *Proc. IEEE Power Energy Soc. Gen. Meeting (PESGM)*, Jul. 2016, pp. 1–5.

[13] S. Han, "Selecting an effective ESS installation location from the perspective of reactive power," *IEEE Access*, vol. 8, pp. 51945–51953, 2020.

[14] D. Das, *Electrical Power Systems*. Chennai, India: New Age International, 2007.

[15] B. R. Gupta, *Power System*. New Delhi, India: S. Chand Publishing, 2008.

[16] Y. Venu, T. Nireekshana, and B. Phanisaikrishna, "Mitigation of Ferranti Effect using thyristor controlled reactor," in *Advances in Automation, Signal Processing, Instrumentation, and Control*. Springer, 2021, pp. 2533–2545.

[17] N. R. Ahire and V. Dake, "Analysis of voltage profile, It's issues and mitigation techniques used in western regional grid of India," in *Proc. 4th Int. Conf. Adv. Electr., Electron., Inf., Commun. Bio-Informat. (AEEICB)*, Feb. 2018, pp. 1–5.

[18] H. A. A. Riyami, A. G. A. Busaidi, A. A. A. Nadabi, M. N. A. Sayabi, A. S. A. Omairi, and O. H. Abdalla, "Impact of installation of 400 kV shunt reactors on Oman grid," in *Proc. 53rd Int. Univ. Power Eng. Conf. (UPEC)*, Sep. 2018, pp. 1–6.

[19] G. Deb, "Ferranti effect in transmission line," *Int. J. Electr. Comput. Eng.*, vol. 2, no. 4, pp. 447–451, 2012.

[20] A. Elansari, J. Burr, S. Finney, and M. Edrah, "Optimal location for shunt connected reactive power compensation," in *Proc. 49th Int. Univ. Power Eng. Conf. (UPEC)*, Sep. 2014, pp. 1–6.

[21] B. Ismail, N. I. A. Wahab, M. L. Othman, M. A. M. Radzi, K. N. Vijyakumar, and M. N. M. Naain, "A comprehensive review on optimal location and sizing of reactive power compensation using hybrid-based approaches for power loss reduction, voltage stability improvement, voltage profile enhancement and loadability enhancement," *IEEE Access*, vol. 8, pp. 222733–222765, 2020.

[22] J. Dixon, L. Moran, J. Rodriguez, and R. Domke, "Reactive power compensation technologies: State-of-the-art review," *Proc. IEEE*, vol. 93, no. 12, pp. 2144–2164, Dec. 2005.

[23] H. Amreiz, A. Janbey, and M. Darwish, "Simulation of HVAC transmission line," in *Proc. 54th Int. Univ. Power Eng. Conf. (UPEC)*, Sep. 2019, pp. 1–6.

[24] T. Gonen, *Modern Power System Analysis*. Boca Raton, FL, USA: CRC Press, 2013.

[25] H. Saadat, *Power System Analysis*. New York, NY, USA: McGraw-Hill, 1999.

[26] J. D. Glover, M. S. Sarma, and T. Overbye, *Power System Analysis & Design*. Boston, MA, USA: Cengage Learning, 2012.

[27] D. Rajicic and A. Bose, "A modification to the fast decoupled power flow for networks with high R/X ratios," *IEEE Trans. Power Syst.*, vol. PWRS-3, no. 2, pp. 743–746, May 1988.

[28] B. N. Mali, P. M. Aglawe, S. A. Mane, and M. Shakya, "Performance study of transmission line Ferranti effect and fault simulation model using MATLAB," *Int. J. Innov. Res. Electr. Electron. Instrum. Control Eng.*, vol. 4, no. 4, pp. 49–52, 2016.

[29] E. Nashawati, N. Fischer, B. Le, and D. Taylor, "Impacts of shunt reactors on transmission line protection," in *Proc. 38th Annu. Western Protective Relay Conf.*, 2011, pp. 1–16.

[30] N. M. Tabatabaei, A. J. Aghbolaghi, N. Bizon, and F. Blaabjerg, *Reactive Power Control in AC Power Systems: Fundamentals and Current Issues* (Power Systems). 2017.

[31] R. M. Mathur and R. K. Varma, "Reactive power control in electrical power transmission systems," in *Thyristor-Based FACTS Controllers for Electrical Transmission Systems*. Piscataway, NJ, USA: IEEE, 2002, pp. 16–39.

[32] J. Hu, P. Yuan, X. Li, and Y. Liu, "Analysis on the necessity of high-voltage shunt reactors in power grid," in *Proc. 10th Int. Conf. Power Energy Syst. (ICPES)*, Dec. 2020, pp. 83–87.

[33] T. K. Nagsarkar and M. S. Sukhija, *Power System Analysis*. London, U.K.: Oxford Univ. Press, 2014.

[34] D. P. Kothari and I. J. Nagrath, *Modern Power System Analysis*. New York, NY, USA: McGraw-Hill, 2003.

[35] A. R. Al-Roomi. (2015). Power flow test systems repository. Halifax, NS, Canada. Accessed: Jun. 14, 2022. [Online]. Available: https://al-roomi.org/power-flow

[36] R. Christie. (1993). Power systems test case archive. University of Washington. Accessed: Jun. 13, 2022. [Online]. Available: https://labs.ece.uw.edu/pstca/pf30/pg_tca30bus.htm

[37] W. Wiechowski and P. B. Eriksen, "Selected studies on offshore wind farm cable connections—Challenges and experience of the Danish TSO," in *Proc. IEEE Power Energy Soc. Gen. Meeting Convers. Del. Electr. Energy 21st Century*, Jul. 2008, pp. 1–8.

**TAREQ FOQHA** received the bachelor's degree in electrical engineering from Palestine Technical University–Kadoorie, Tulkarm, Palestine, in 2020. He is currently pursuing the M.Sc. degree in electrical power engineering with An-Najah National University. He is also a Lecturer of engineering with the Faculty of Engineering and Technology, Palestine Technical University–Kadoorie. His research interests include power system control, computer applications in power engineering, power system protection, and power system security.

**SHADY S. REFAAT** (Senior Member, IEEE) received the B.A.Sc., M.Sc., and Ph.D. degrees in electrical engineering from Cairo University, Giza, Egypt, in 2002, 2007, and 2013, respectively. He has worked in industry for more than 12 years as an Engineering Team Leader, a Senior Electrical Engineer, and an Electrical Design Engineer on various electrical engineering projects. He is an Associate Research Scientist with the Department of Electrical and Computer Engineering, Texas A&M University at Qatar. He is a member of the Institution of Engineering and Technology (IET) and the Smart Grid Center–Extension in Qatar (SGC-Q). He has published more than 150 journals and conference papers and one book. His principal work area focuses on electrical machines, power systems, smart grids, big data, energy management systems, reliability of power grids and electric machinery, fault detection, condition monitoring, and development of fault-tolerant systems. Also, he has participated in and led several scientific projects over the last eight years. He has successfully realized many potential research projects.

**SAMER ALSADI** (Senior Member, IEEE) received the M.Sc. degree in power systems from the Mendeleyev University of Chemical Technology of Russia, Moscow, in 1996, and the Ph.D. degree in electrical and power transmission installation/installer, general from the Moscow Power Engineering Institute (Technical University). He worked as a Consultant in Jenin's municipality for one year. He is currently an Associate Professor with the Electrical Engineering Department, Faculty of Engineering and Technology, Palestine Technical University–Kadoorie, Tulkarm, Palestine. His research interests include mesh networking, network and systems, protection systems, and forecasting.

**KAIS ABDULMAWJOOD** (Senior Member, IEEE) received the B.Sc. degree in electrical engineering from Baghdad University, and the M.Sc. degree in electric engineering, electronics and communication from Al-Mustansiriya University, in 1998. He is currently pursuing the Ph.D. degree in electrical engineering with the University of Ontario Institute of Technology, ON, Canada. He works as a Laboratory Manager in the Electrical and Computer Engineering Program, Texas A&M University at Qatar. Prior to joining Texas A&M University at Qatar, in 2007, he worked as the Head of the Computer Center, Al-Mustanisriya University. He also served as a Scientific Coordinator with the Computer and Software Engineering Department, Faculty of Engineering. While at Al-Mustansirya University, he served as an Adjunct Lecturer of computer science and information technology with the University of Technology, Iraq, and a Visiting Lecturer with the Computer College, Thimar University, Yemen.

• • •